Transaction B: Mechanical Engineering
Vol. 17, No. 2, pp. 146–156

Research Note

SCIENTIA IRANICA

Dynamic Response of Floating Wind Turbine

M. Karimirad[1]

Abstract. *Like other offshore structures, floating wind turbines are subjected to stochastic wave and wind loads that cause a dynamic response in the structures. Wind turbines should be designed for different conditions, such as Operational and Survival conditions. In high sea states, the response can be quite different from the operational condition. The present paper deals with coupled wave and wind induced motion in harsh conditions, up to 15 m significant wave height and 50 m/sec average wind speed. There are several ways to deal with the dynamic response of floating wind turbines. The Coupled Time domain dynamic response analysis for a moored spar wind turbine subjected to wave and wind loads is carried out using DeepC. DeepC is well known software for calculating the coupled dynamic response of moored floating structures. The aerodynamic forces on a parked wind turbine are calculated, based on the strip theory, and imported to the DeepC through a MATLAB interface. At each time step, the relative wind velocity, based on the response of the structure, is calculated.*

Keywords: *Offshore; Floating wind turbine; Stochastic dynamic response; Aero-hydro-elastic.*

INTRODUCTION

The first accepted establishment of the use of wind turbines was in the tenth century in Persia [1]. With the advent of the industrial era, wind mills were practically relegated to pump water for agricultural use. In the 20th century, new designs enabled electricity generation [2]. Denmark, Germany, Holland and the USA had a great influence on the development of wind turbines [3]. The increasing demand for energy, global warming, air and other pollutions, safety, cost, and the large amount of energy found in waves and wind, have motivated the search for renewable energy sources. The UK, Japan, Norway, Sweden, France and the USA were pioneers. For more information, refer to Ocean Wave Energy Conversion by McCormick [4]. Day by day, the demand for energy has increased. The European Union has a target to make 22.1% of its electricity by 2020 from renewable energy, as in the Kyoto protocol [5]. Vast deepwater wind resources represent the potential use of floating offshore wind turbines to power much of the world with renewable energy [6]. In Figure 1, some floating wind turbine proposed concepts have been shown. Currently, there is a number of offshore wind turbine floating foundation concepts in various stages of development. They fall into three main categories: Spars, Tension Leg Platforms (TLP's) and semi-submersible/hybrid systems. In general terms,

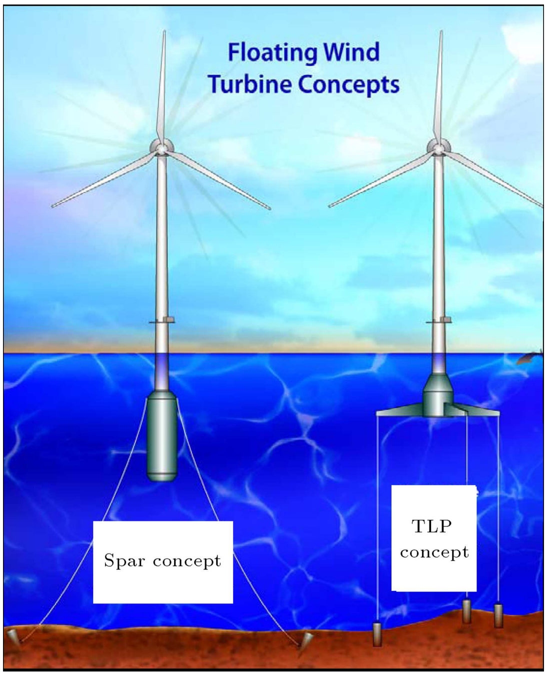

Figure 1. Floating support platform concepts for offshore wind turbines [7].

1. *Centre for Ships and Ocean Structures (CeSOS), Norwegian University of Science and Technology (NTNU), P.O. Box-7491 Trondheim, Norway. E-mail: madjid.karimirad@ntnu.no*

Received 28 February 2009; received in revised form 24 July 2009; accepted 24 November 2009

the spars type has a better heave performance than semisubmersibles due to its deep draft and reduced vertical wave exciting forces [7].

Larsen and Hanson [8] have done some studies on floating wind turbines under operational conditions. In the present research, a parked turbine due to wave and wind load will be analyzed under harsh conditions. A floating wind turbine is a new technology and little work has been done regarding its response under harsh environmental conditions.

COUPLED DYNAMIC RESPONSE

The floating offshore wind turbine is a new challenging technology. In offshore technology, analyzing the dynamic response of floating structures has been developed [9]. In this study, a coupled hydro-aero dynamic response analysis of a catenary moored spar floating wind turbine is carried out. DeepC [10], software for calculating the dynamic response of moored floating structures, has been used. A nonlinear FEM model of mooring lines including clump weight has been modeled for large deflections. In a coupled analysis, the complete system of equations accounting for the rigid body model of the floater, as well as the slender body model for mooring lines, is solved simultaneously using a non-linear time domain approach for dynamic analysis. Dynamic equilibrium is obtained at each time step ensuring consistent treatment of the floater/slender structure coupling effects. The equation of motion of a floating structure in the time domain can be written as follows [11]:

$$M\ddot{x} + C\dot{x} + D_1\dot{x} + D_2 f(\dot{x}) + K(x)x = q(t, x, \dot{x}), \tag{1}$$

$$\begin{aligned} &M = m + A(\omega), \quad A(\omega) = A_\infty + a(\omega), \\ &A_\infty = A(\omega = \infty), \quad C(\omega) = C_\infty + c(\omega), \\ &C_\infty = C(\omega = \infty), \end{aligned} \tag{2}$$

where:

- M: frequency-dependent mass matrix,
- m: body mass matrix,
- A: frequency-dependent added-mass,
- C: frequency-dependent potential damping matrix,
- D_1: linear damping matrix,
- D_2: quadratic damping matrix,
- f: vector function where each element is given by $f_i = \dot{x}_i|\dot{x}_i|$,
- K: (position-dependent) hydrostatic stiffness matrix,
- x: position vector,
- q: exciting force vector.

One of the most frequently used methods for solving Equation 1 is based on the convolution integral which is introduced here. Now, we consider frequency-dependent coefficients (radiation part of the problem) [12,13].

$$\mathrm{RF}(t) = A(\omega)\ddot{x} + C(\omega)\dot{x}. \tag{3}$$

Assuming that radiation force varies sinusoidally at one single frequency, we can write the equation in the frequency domain:

$$\begin{aligned} \mathrm{RF}(\omega) &= (-\omega^2 A(\omega) + i\omega C(\omega))X(\omega) \\ &= (i\omega A(\omega) + C(\omega))i\omega X(\omega). \end{aligned} \tag{4}$$

Using Equation 2, we can write:

$$\mathrm{RF}(\omega) = -\omega^2 A_\infty X(\omega) + [i\omega a(w) + c(\omega)]i\omega X(\omega). \tag{5}$$

Applying the inverse Fourier transform:

$$\mathrm{RF}(t) = A_\infty \ddot{x}(t) + \int_{-\infty}^{\infty} h(t-\tau)\dot{x}(\tau)d\tau. \tag{6}$$

Physically, values of $h(t-\tau)$ for, $t < 0$ are zero. Causality implies that $h(t-\tau) = 0$ for $\tau > t$. So, we can write Equation 6 as:

$$\mathrm{RF}(t) = A_\infty \ddot{x}(t) + \int_{0}^{t} h(t-\tau)\dot{x}(\tau)d\tau. \tag{7}$$

Substituting the RF(t) in Equation 1:

$$\begin{aligned} &(m + A_\infty)\ddot{x} + D_1\dot{x} + D_2 f(\dot{x}) + K(x)x \\ &\qquad + \int_{0}^{t} h(t-\tau)\dot{x}(\tau)d\tau = q(t, x, \dot{x}), \end{aligned} \tag{8}$$

where $h(\tau)$, the retardation function, is computed by a transform of the frequency-dependent added-mass and damping:

$$h(\tau) = \frac{1}{2\pi}\int_{-\infty}^{\infty} (c(\omega) + i\omega a(\omega))\exp(i\omega t)d\omega. \tag{9}$$

Using $c(\omega) = c(-\omega)$ and $a(\omega) = a(-\omega)$:

$$h(\tau) = \frac{1}{\pi}\int_{0}^{\infty} (c(\omega) + \cos(\omega\tau) - \omega a(\omega)\sin(\omega\tau))d\omega. \tag{10}$$

From causality, the two parts in the integral for $\tau < 0$ must be opposite, and for $\tau > 0$, identical. Mathematically it means:

$$h(\tau) = \frac{2}{\pi}\int_0^\infty c(\omega)\cos(\omega\tau)d\omega. \quad (11)$$

Based on this equation, the retardation function can be found using potential damping, $c(\omega)$. We have to form Equation 8 for our problem. First, the excitation forces should be found based on the Panel Method in HydroD [14]. The HydroD solves the potential theory using the WADAM/WAMIT solver [15]. WAMIT [16] can be used for finding the excitation forces. Nonlinear quadratic viscous damping (Morison type) can be added to the equation of motion in DeepC also. The relative velocity of water particles and the platform motion are considered for calculating the viscous forces. The mooring line forces, as well as wind forces, will be added to the right hand side of Equation 8 at each time step. The solution of Equation 8 in the time domain is based on an incremental procedure using the dynamic time integration scheme, according to Newmark β family methods. The Newton-Raphson iteration is used to assure equilibrium between internal and external forces at every time step [11].

Wind Force

Wind turbine blades and the tower are long and slender structures. It is, therefore, assumed that in many aerodynamic models, the flow at a given point is two-dimensional and the 2D aerofoil data can, thus, be applied [17]. Increased development in wind turbine aerodynamics has created a demand for more detailed information of non-linear unsteady loads [18]. In the present study, we use a simplified approach to model the aerodynamic forces of the floating wind turbine. Figure 2 illustrates a transversal cut of the blade element. The blade element moves in the airflow at a relative speed, V_{rel}. The lift and drag coefficients are [2]:

$$C_L(\alpha) = \frac{f_L}{\frac{1}{2}\rho V_{\text{rel}}^2 c}, \text{ and } C_D(\alpha) = \frac{f_D}{\frac{1}{2}\rho V_{\text{rel}}^2 c}, \quad (12)$$

where:

- f_D: drag force,
- f_L: lift force,
- c: chord,
- ρ: air density,
- α: angle of attack,
- V_{rel}: relative velocity.

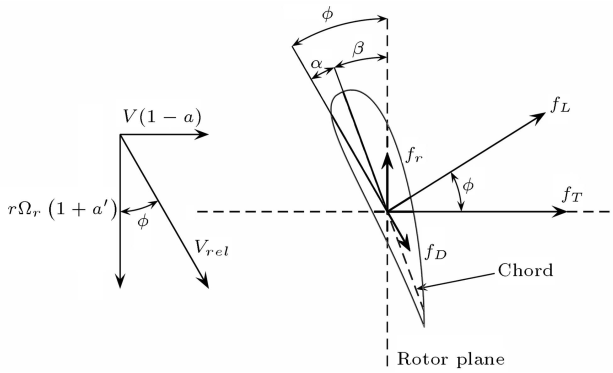

Figure 2. Forces on a blade element [2].

$$V_{\text{rel}} = V\sqrt{(1-a)^2 + \left(\frac{r\Omega_r}{V}(1-a')\right)^2}, \quad (13)$$

$$\alpha = \phi - \beta, \quad (14)$$

$$\tan(\phi) = \frac{V}{r\Omega_r}\frac{1-a}{1+a'}, \quad (15)$$

where:

- a' and a: axial and rotational induction factors, respectively,
- V: upstream wind velocity,
- f_T: total force on airfoil,
- r: distance of airfoil section from blade root,
- Ω_r: rotational velocity (rad/sec).

In order to maximize the power, it is necessary to have the relation between a' and a as [17]:

$$a' = \frac{1-3a}{4a-1}. \quad (16)$$

At each time step, the motion of the system has been used to calculate the relative wind force for each element of the blades and the tower of the wind turbine. The coupling has been done through a MATLAB-based routine. In Equation 17, the simple relation between relative velocity and the wind force has been defined to show the role of the wind force in changing the equation of motion. Using Equation 12, after some simplification, we can define the wind force as a function of relative wind velocity. In Equation 17, this relation has been shown.

$$F_{\text{wind}} \propto U_{RH}^2 = (V_H - L\dot{\eta}_5\cos\eta_5 - \dot{\eta})^2,$$

$$F_{\text{wind}} \propto V_H^2 + (L\dot{\eta}_5\cos\eta_5)^2 + \dot{\eta}_1^2 - 2V_H L\dot{\eta}_5\cos\eta_5 - 2V_H\dot{\eta}_1 + 2L\dot{\eta}_5\dot{\eta}_1\cos\eta_5, \quad (17)$$

where:

F_{wind}: wind force applied on the structure,
U_{RH}: relative horizontal wind velocity,
V_H: horizontal velocity of environmental wind (Upstream wind),
L: nacelle elevation from mean water level surface,
η_5: pitch motion response of platform,
η_1: surge motion of the platform.

By neglecting second order and higher order platform velocity components, we end up with Equation 18.

$$F_{\text{wind}} \propto V_h^2 - 2V_H L\dot{\eta}_5 \cos\eta_5 - 2V_H\dot{\eta}_1. \tag{18}$$

The last two terms are damping, which can be added to the left hand side of the equation of motion (Equations 1 and 8). The damping depends on time because of stochastic wind and motion. By doing coupled analysis, this aerodynamic damping shows itself in reducing the resonance response (refer to Conclusion).

System (Offshore Floating Wind Turbine)

In this paper, we focus on a Floating Wind Turbine based on a Catenary Moored Spar Platform. The NREL 5 MW [19] Wind Turbine has been chosen and mounted on a 120 meters draft spar platform (Figure 3). In Table 1, the properties of the wind turbine have been listed. The wind turbine tower, at the base, has the diameter of 6 m and thickness of 0.027 m. At the top, it has the diameter of 3.87 m and thickness of 0.019 m [19]. In Table 2, the blade structural properties and, in Table 3, the blade aerodynamic properties have been listed. The spar (platform) characteristics have been listed in Table 4.

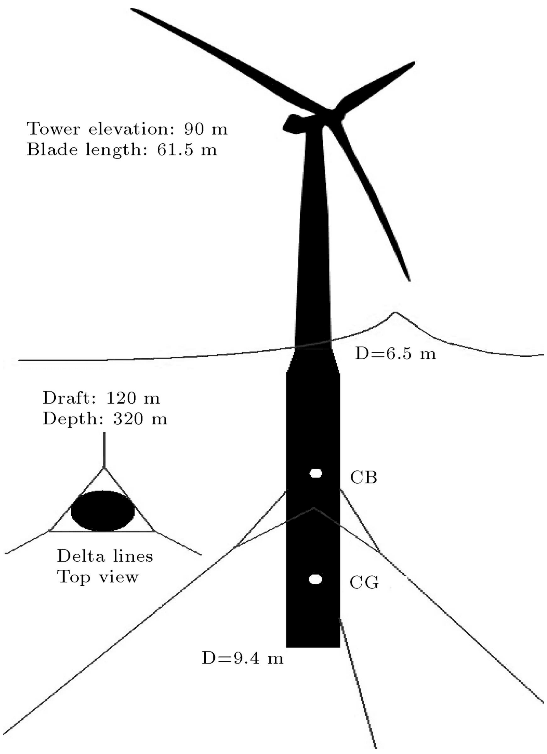

Figure 3. Spar floating wind turbine.

Environmental Condition

Wave and wind climate are correlated, because waves are usually wind-generated. The correlation between wave data and wind data must be accounted for in the design of a floating wind turbine. In the present study, a 100-year return period of winds and waves is considered to investigate the 100-year motion response of a floating wind turbine.

The representative site for a floating wind turbine has been chosen in open seas in the Northern North

Table 1. NREL 5-MW wind turbine properties [19].

Rating	5 MW
Rotor Orientation, Configuration	Upwind, 3 blades
Rotor, Hub Diameter	126 m, 3 m
Hub Height	90 m
Cut-In, Rated, Cut-Out Wind Speed	3 m/s, 11.4 m/s, 25 m/s
Rotor Mass	110,000 kg
Nacelle Mass	240,000 kg
Tower Mass	347,460 kg

Table 2. Blade structural properties [19].

Length	61.5m
Overall (Integrated) Mass	17,740 kg
Second Mass Moment of Inertia	11,776,047 kgm^2
First Mass Moment of Inertia	363,231 kgm

Table 3. Blade aerodynamic properties [19].

Section	Airfoil
1 and 2	Cylinder 1
3	Cylinder 2
4	DU40_A17
5 and 6	DU35_A17
7	DU30_A17
8 and 9	DU25_A17
10 and 11	DU21_A17
12, 13, 14, 15, 16 and 17	NACA64_A17

Table 4. Spar (platform) characteristics.

Total Draft	120 m
Diameter Above Taper	6.5 m
Diameter Below Taper	9.4 m
Mass, Including Ballast	7593,000 kg
Centre of Gravity, CG	-92.58 m
Roll/Pitch Inertia about CG	4.489E+09 kgm^2
Yaw Inertia about Centerline	1.672E+08 kgm^2

Sea. A 100-year significant wave height of 15 m and peak period of 19 sec have been chosen [20]. It is mentioned in NORSOK N-003 that the average wind velocity at 10 m above sea level, the characteristic value with an annual probability of exceedance of 0.01, can be chosen as 41 m/s (10 min average) for the whole continental shelf of Norway [21]. This wind velocity is higher compared to that found from empirical formula, such as in Beaufort [22]. The wind field is characterized by shear, which is dependent on roughness. Using the logarithmic wind speed profile (Equation 19), the mean wind speed at 10 m can be transformed to the mean wind speed at the tower top [23].

$$\frac{\nu(z)}{\nu(h)} = \frac{\ln(\frac{z}{z_0})}{\ln(\frac{h}{z_0})}, \tag{19}$$

where z is the height and z_0 is the roughness parameter, which depends on wind speed, distance from land, water depth and wave field for offshore sites. The roughness parameter varies from 0.0001 for a calm sea to 0.003 in coastal areas with onshore wind. Under harsh environmental conditions, the roughness parameter can be chosen as 0.0003 to make a realistic result. Using Equation 19, the mean wind speed at the top of the tower (10 min average) is 50 m/sec. Turbulent wind consists of longitudinal, lateral and vertical components [3]. Turbulence intensity is the basis of measuring turbulence and is defined as the variance of wind velocity over the mean wind speed during a specified time period [17]. In Figure 4, turbulence intensity, according to various standards, has been shown [24]. In our study, turbulence intensity is chosen to be 0.2.

TurbSim from NREL has been used in order to generate turbulent wind. TurbSim is a stochastic, full-field, turbulent-wind simulator. It numerically simulates the time series of three-dimensional wind velocity vectors at points in a vertical rectangular grid [25]. The IEC Spectral Model (Kaimal spectrum) has been used in order to generate turbulent wind. The time series from the Kaimal spectrum (Equation 20) is constructed based on inverse DFT (Discrete Fourier Transform) [17].

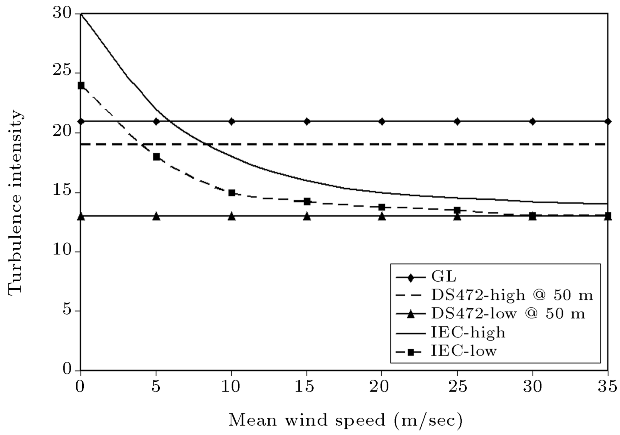

Figure 4. Turbulence intensity [24].

$$S(f) = \frac{I^2 V_{10\,\mathrm{min}} l}{(1 + 1.5\frac{f.l}{V_{10\,\mathrm{min}}})^{5/3}}, \tag{20}$$

where:

$S(f)$:	power spectral density,
f:	frequency (Hz),
I:	turbulence intensity,
l:	length scale,
$V_{10\,\mathrm{min}}$:	10 min averaged mean wind speed.

The wind speed time history is generated at the top of the tower. The wind velocity at other points (blades and tower elements) has been constructed by considering the shear boundary layer which has been discussed previously, but the coherence between different grids has not been considered in the present study [17,24].

Different Load Cases

In IEC standard, the load cases are defined for eight situations: power production, power production plus fault, start up, normal shut down, emergency shutdown, parked, parked plus fault and transport, assembly, maintenance and repair [3]. Under harsh environmental conditions, the wind turbine is parked. A parked condition is a non-operational machine state [24]. The wind is acting perpendicular to the nacelle, i.e. with a full drag on the nacelle, and the blades are pitched to give a full drag also on the blades [23]. For pitch regulated wind turbines, a critical non-operational condition occurs when the wind is from the front, one of the blades is vertical and the load results from the blade lift [24]. In this research, we focus on the full drag case. Different load cases have been chosen to investigate and compare the effect of wind and wave loading on the coupled dynamic response of the floating wind turbine. In Table 5, we have summarized the load cases which we have performed. As we have avoided the Mathieu instability, the heave motion is not very important

Table 5. Load cases.

No.	Description
1	Just wave
2	Wave and constant wind force
3	Wave and steady wind (considering relative motion of spar platform)
4	Wave and turbulent wind (considering relative motion of spar platform)

for our case. The Mathieu instability for a spar platform arises when there is a harmonic variation in the pitch restoring coefficients caused by large heave motion [26,27].

DYNAMIC MOTION RESPONSES

Response of the System (Just Wave)

The wave induced response has been carried out. The PM spectrum with significant wave height of 15 m and peak period of 19 sec has been chosen. In Figures 5 and 6, the time history and spectrum of the pitch and surge motion have been plotted.

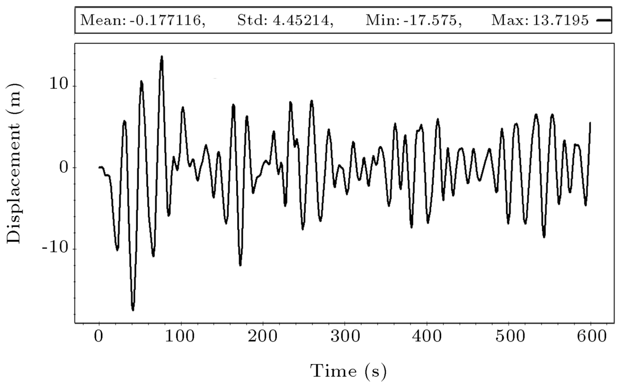

Figure 5a. Time history of surge motion (just wave induced case).

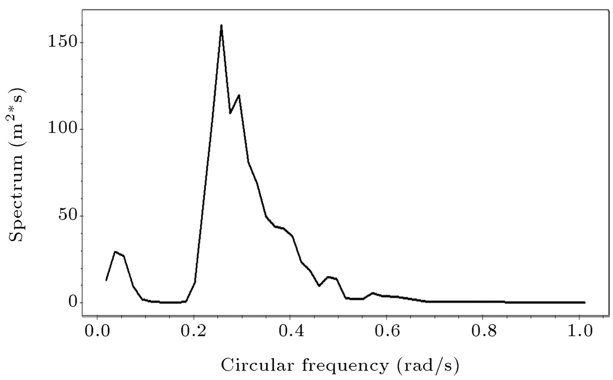

Figure 5b. Spectrum of surge motion (just wave induced case).

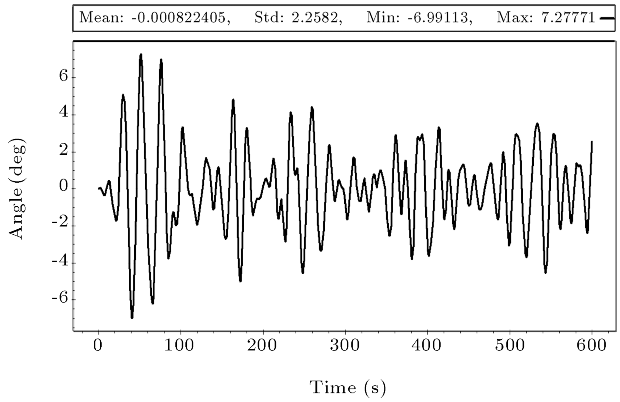

Figure 6a. Time history of pitch motion (just wave induced case).

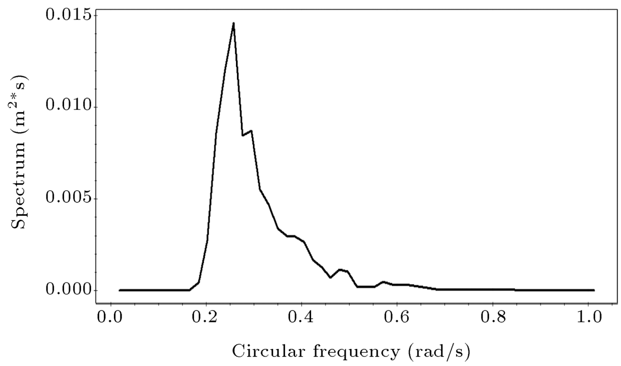

Figure 6b. Spectrum of pitch motion (just wave induced case).

Response of System (Wave and Constant Wind Load)

We have applied constant wind force at the top of the tower. The same PM Spectrum as before has been chosen. A steady wind with a velocity of 50 m/sec has been defined. This wind makes a constant force of 2.1042E+6 N at the top of the tower. In Figures 7 and 8, the time history and spectrum of surge and pitch motions are plotted, respectively. Comparing the results with previous analyses (without wind, just wave), it is obvious that constant force has made no contribution to the dynamic amplitude of the response, but it has increased the mean of the pitch and surge response.

Response of the System (Wave and Steady Wind)

In this section, we have applied the same PM Spectrum as before and, with a steady wind, considered the relative motion of the platform. Considering the motion of the platform in relative velocity (Equation 17) makes some aerodynamic damping. In Figure 9, the time history and spectrum of the wind force corrected

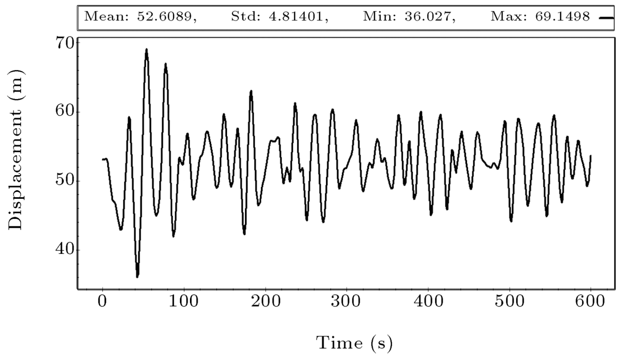

Figure 7a. Time history of surge motion (wave and constant windload case).

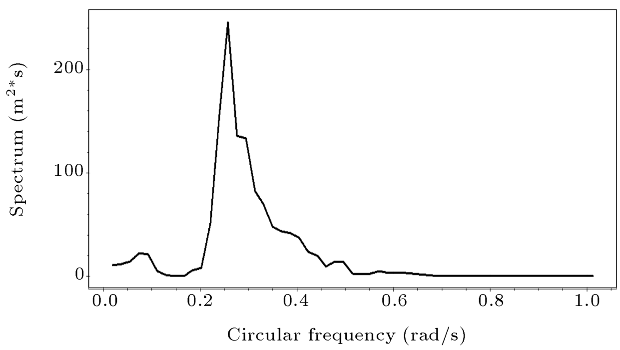

Figure 7b. Spectrum of surge motion (wave and constant wind load case).

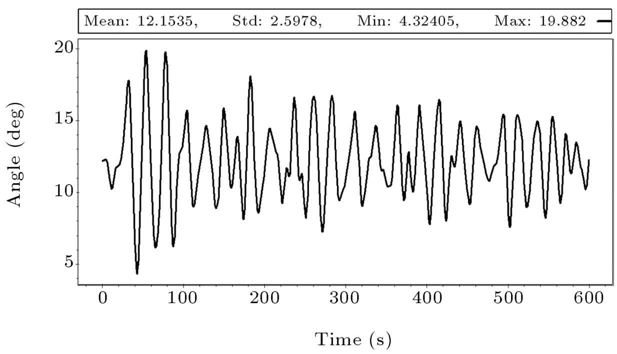

Figure 8a. Time history of pitch motion (wave and constant wind load case).

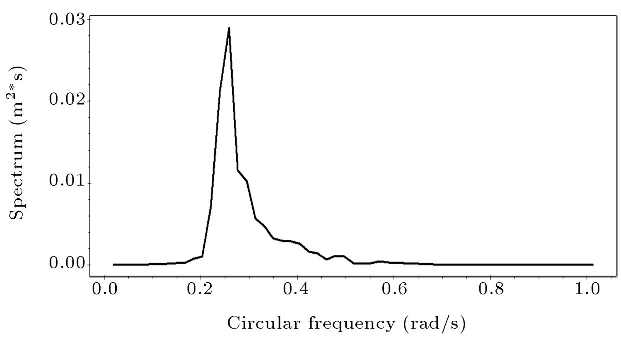

Figure 8b. Spectrum of pitch motion (wave and constant wind load case).

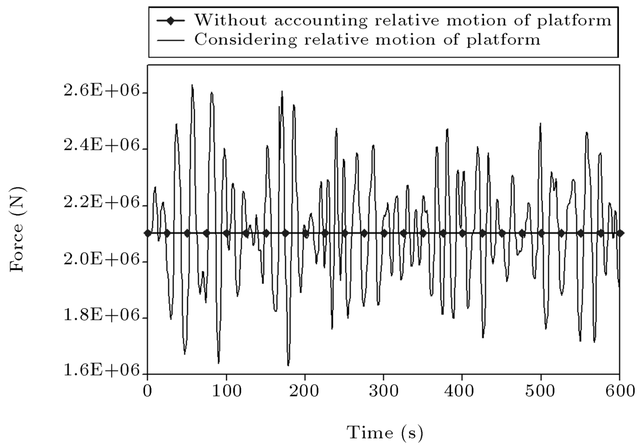

Figure 9a. Time history of wind force.

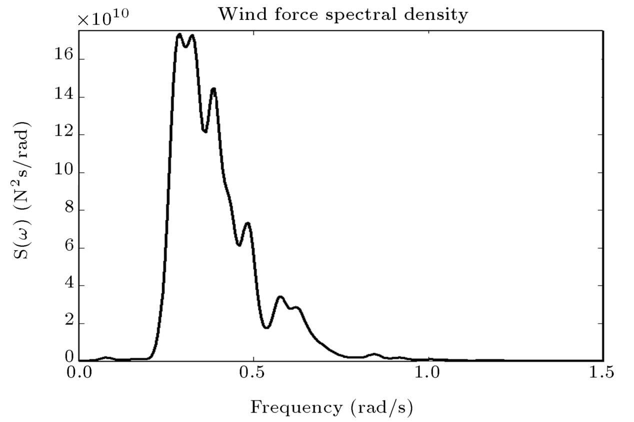

Figure 9b. Spectrum of wind force.

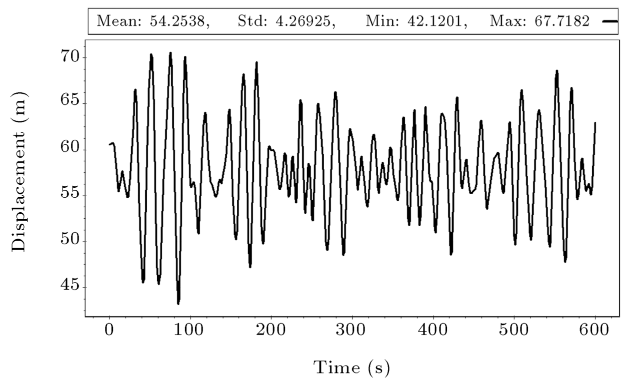

Figure 10a. Time history of surge motion (wave and steady wind case).

by considering relative wind velocity based on platform motion, has been plotted.

In Figures 10 and 11, the time history and spectrum of the surge and pitch motion of the system (floating wind turbine) has been plotted. The role of aerodynamic damping in decreasing the dynamic amplitude of the motion is obvious. The mean of the motions has not been changed and is almost the same as the case with constant wind force.

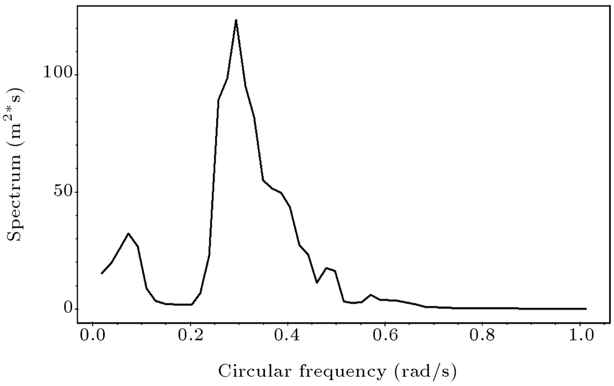

Figure 10b. Spectrum of surge motion (wave and steady wind case).

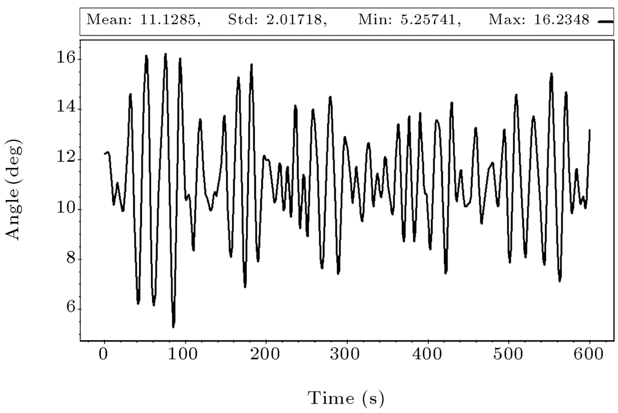

Figure 11a. Time history of pitch motion (wave and steady wind case).

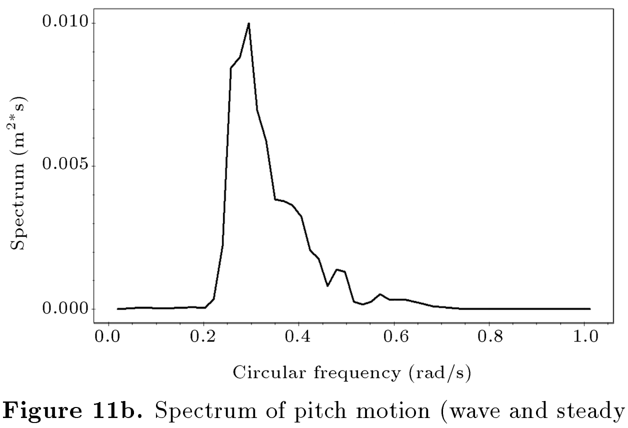

Figure 11b. Spectrum of pitch motion (wave and steady wind case).

General Case (Wave and Turbulent Wind)

We have considered waves and turbulent wind. The relative wind velocity has been corrected considering platform motions to find the accurate wind force at each time step and then input through a MATLAB interface routine to the DeepC. The PM Spectrum with significant wave height of 15 m and peak period of 19 sec related to a one hundred year return period has

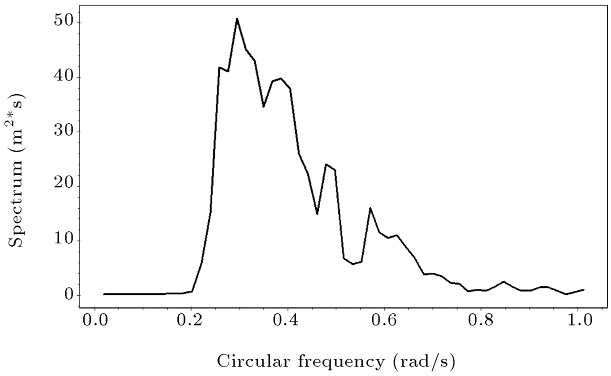

Figure 12a. Wave spectrum.

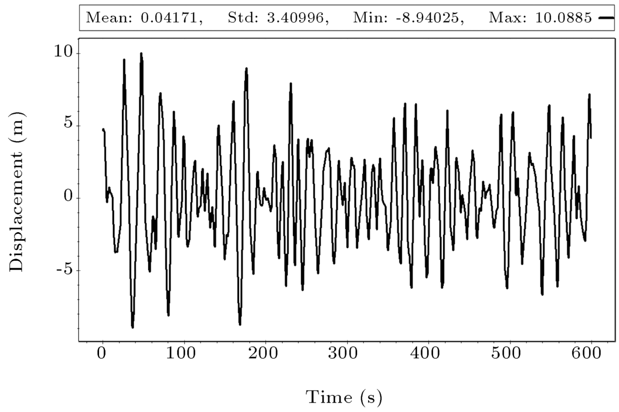

Figure 12b. Time history of wave elevation.

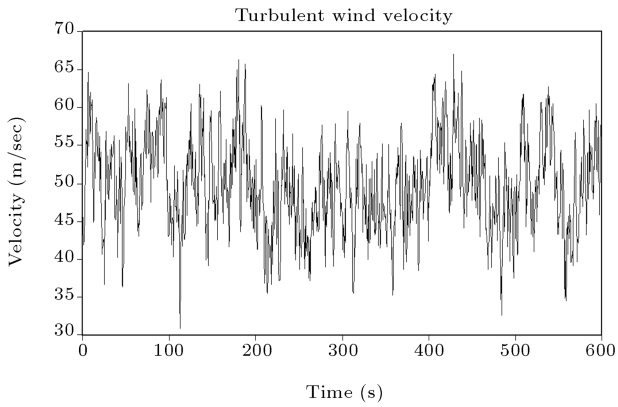

Figure 13a. Time history of turbulent wind velocity (general case, wave and turbulent wind).

been plotted in Figure 12a. In Figure 12b, the wave elevation time history has been plotted.

The turbulent wind time history with a mean of 50 m/sec and 0.2 turbulence intensity has been plotted in Figure 13a. Wind has some low frequency part (Figure 13b) that can excite the low natural frequency of the structure. In fact, in the design of floating offshore structures, we try to place the natural frequency of the system far away from the wave frequency part to avoid the resonant response.

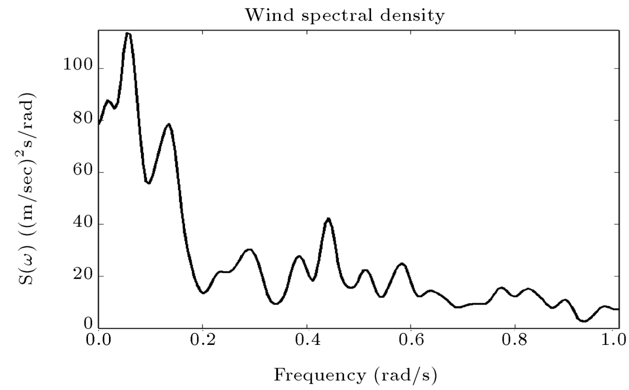

Figure 13b. Spectrum of turbulent wind velocity (general case, wave and turbulent wind).

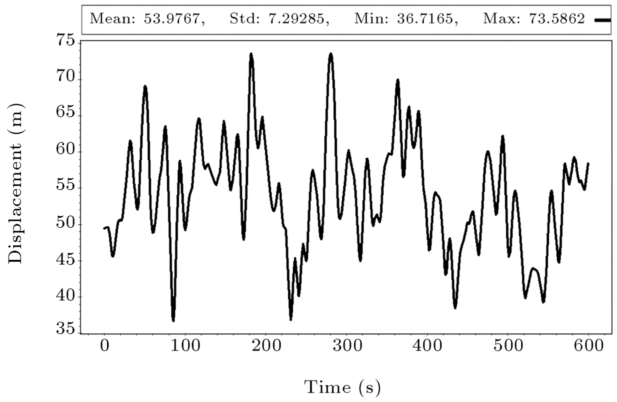

Figure 14a. Time history of surge motion (general case, wave and turbulent wind).

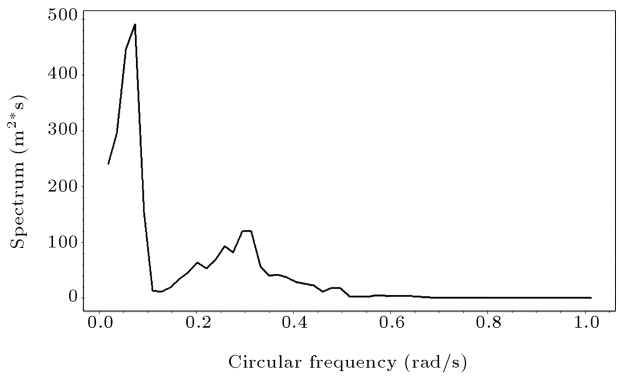

Figure 14b. Spectrum of surge motion (general case, wave and turbulent wind).

In Figures 14 and 15, the time history and spectrum of the surge and pitch motion of the system has been plotted. The pitch and surge natural frequencies have been excited by turbulent wind.

As the aerodynamic damping in a parked turbine is less than for an operating turbine, the introduction of more hydrodynamic damping can decrease the pitch resonance response. Fin-like structures called strakes, attached in a helical fashion around the exterior of

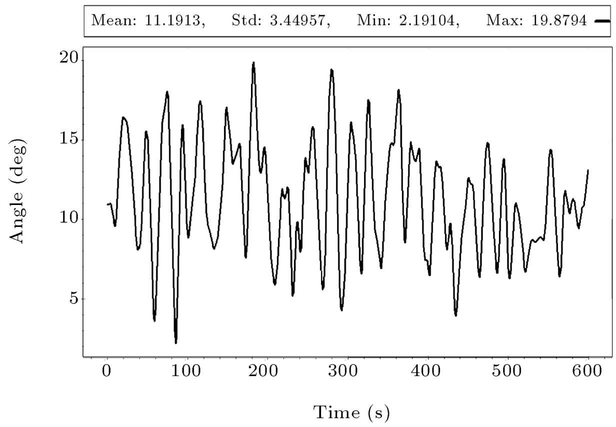

Figure 15a. Time history of pitch motion (general case, wave and turbulent wind).

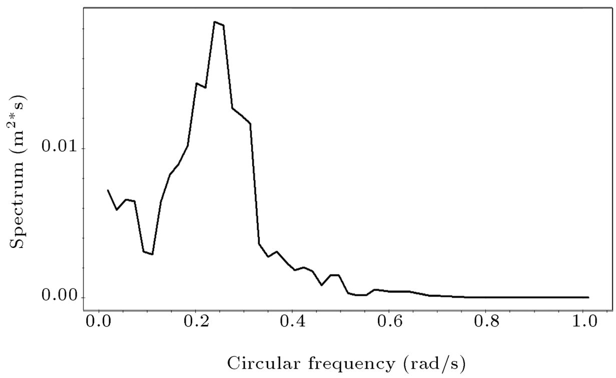

Figure 15b. Spectrum of pitch motion (general case, wave and turbulent wind).

the cylinder, act to break the water flow against the structure [28].

We remember that under harsh conditions, the wind turbine is parked and there is no power generation. Under non-operating conditions (harsh environmental conditions), the main goal is to keep the platform safe through the storm/ hurricane. The response of the floating wind turbine under such extreme and harsh environmental conditions is reasonable and the motions are acceptable. The maximum pitch motion is around 20 degrees. The air gap between the blade tip and the water wave crest can be calculated as:

$$AG = (\text{calm water gap}) \times \cos(\text{pitch motion})$$

$$-\text{max.wave crest height},$$

$$AG = (90 - 61.5) \times \cos(20\,\text{deg.}) - 10 = 16.7\,\text{m}. \quad (21)$$

In the above load cases, we have seen resonance around natural frequencies. Resonance should not be confused with instability. Resonant motion requires external excitation and grows linearly. Also, in a resonance, the frequency of the external excitation coincides with one of the system's natural frequencies [29].

CONCLUSION

Floating wind turbines are a new technology in the offshore wind industry. We have arranged different load conditions to see the effect of different loads on the response. We can conclude some of our results as follows:

a) For constant wind without turbulence, the dynamic motion will be decreased compared to the same model without applying wind (just wave).

b) For turbulent wind, the damping is dependent on wind frequency. The wind force can excite the natural frequency of the pitch and surge motion and cause some resonance response.

c) By performing a coupled analysis, we can see aerodynamic damping, which decreases the dynamic motion. Previously, Karimirad [30] performed an uncoupled analysis for a floating wind turbine and showed the necessity of doing a coupled analysis.

d) Pitch motion damping is due to wind and wave (similar importance).

e) A great resonance for surge wind induced motion can be seen under harsh condition. For the surge response, wave damping is less than wave damping for a pitch motion (the wave damping is proportional to the frequency).

f) Introducing more hydrodynamic viscous damping can decrease the resonant response.

ACKNOWLEDGMENT

The author would like to thank Prof. Torgeir Moan and Dr Zhen Gao from CeSOS, NTNU, Norway.

REFERENCES

1. Spera, D.A., *Wind Turbine Technology, Fundamental Concepts of Wind Turbine Engineering*, pp. 1-46, ASME Press, USA (1998).
2. Bianchi, D.F., Battista, H.D. and Mantz, R.J., *Wind Turbine Control Systems*, pp. 8-30, Springer, Germany (2007).
3. Manwell, J.F., McGowan, J.G. and Rogers, A.L., *Wind Energy Explained, Theory, Design and Application*, pp. 1-20, John Wiley and Sons Ltd, England (2002).
4. McCormick, M.E. *Ocean Wave Energy Conversion*, pp. 1-6, Dover publication, USA (2007).
5. Tempel, V.D.J. "Design of support structures for offshore wind turbines", PhD Thesis, pp. 7-17, Delft University of Technology, Netherland (2006).
6. Jonkman, J.M. and Buhl, J. "Loads analysis of a floating offshore wind turbine using fully coupled simulation", National Renewable Energy Laboratory, PhD Thesis, pp. 1-200, NREL, USA (2007).
7. Roddier, D., Cermelli, C. and Weinstein, A. "Windfloat: A loatong foundation for offshore wind turbines Part I: Design basis and qualification process", OMAE2009-79229, USA (2009).
8. Larsen, T.J. and Hanson, T.D. "A method to avoid negative damped low frequent tower vibrations for a floating, pitch controlled wind turbine", *Journal of Physics*, The Science of Making Torque from Wind, IOP Publishing, Conference Series 75 (2007) 012073, doi:10.1088/1742-6596/75/1/012073 (2007).
9. Homayon Heidari, A., Borghei, S.M. and Sohrabpour, M. "Amic response of a moored semisubmersible in short-crested wave fields", *Scientia Iranica*, **11**(4), pp. 351-360, Sharif University of Technology, Iran (2004).
10. DNV, DET NORSKE VERITAS "DeepC user manual", Norway (2008).
11. MARINTEK "Simo/riflex user manual", Norway (2008).
12. Faltinsen, O.M., *Sea Loads on Ships and Offshore Structures*, pp. 60-62, Cambridge University Press, UK (1995).
13. Falnes, J., *Ocean Waves and Oscillating Systems*, pp. 31-37, Cambridge University Press, USA (2005).
14. DNV, DET NORSKE VERITAS "HydroD user manual", Norway (2008).
15. DNV, DET NORSKE VERITAS "WADAM user manual", Norway (2005).
16. Chakrabarti, S., *Handbook of Offshore Engineering*, pp. 197-277, Elsevier Ltd, UK (2005).
17. Hansen, M.O.L., *Aerodynamics of Wind Turbines*, pp. 26-83, EarthScan, UK (2008).
18. Soltani, M.R. and Rasi Marzabadi, F.B. "Effect of reduced frequency on the aerodynamic behavior of an airfoil oscillating in a plunging motion", *Scientia Iranica, Tranc. B*, **16**(1), pp. 40-52, Iran (2009).
19. Jonkman, J.M. "Dynamics modeling and loads analysis of an offshore floating wind turbine", *National Renewable Energy Laboratory (NREL)*, Technical Report, NREL/TP-500-41958, USA (2007).
20. DNV "Design of offshore wind turbine structures", DNV-OS-J101, Norway (2004).
21. Standards Norway "Actions and action effects", NORSOK N-003, Norway (2007).
22. Beer, T., *Environmental Oceanography*, pp. 59-85, CRC-Press, USA (1997).
23. DNV/Risø "Guidelines for design of wind turbines", 2nd Edn., pp. 180-184, Jydsk Centraltrykkeri, Denmark (2002).
24. Burton, T., Sharpe, D., Jenkins, N. and Bossanyi, E. *Wind Energy Handbook*, pp. 299-301, John Wiley and Sons Ltd, England (2008).

25. Agarwal, P. and Manuel, L. "Simulation of offshore wind turbine response for long-term extreme load prediction", *Journal of Engineering Structures,* **31**, pp. 2236-2246 (2009).

26. Koo, B.J., Kim, M.H. and Randall, R.E. "Mathieu instability of a spar platform with mooring and risers", *Ocean Engineering Journal*, **31**, pp. 2175-2208 (2004).

27. Haslum, H.A. and Faltinsen, O.M. "Alternative shape of spar platform for use in hostile areas", *Offshore Technology Conference*, OTC 10953, USA (1999).

28. Agarwal, A.K. and Jain, A.K. "Nonlinear coupled dynamic response of offshore spar platforms under regular sea waves", *Ocean Engineering Journal*, **30**, pp. 517-551 (2003).

29. Bir, G. and Jonkman, J. "Aeroelastic instabilities of large offshore and onshore wind turbines", *EAWE Torque from Wind Conference*, Denmark (2007).

30. Karimirad, M. "Dynamic response of floating wind turbine (FWT) due to wave and wind loads", Internal Report, CeSOS, NTNU, Norway (2008).

BIOGRAPHY

Madjid Karimirad received his BS and MS degrees from Sharif University of Technology, Tehran, in the mechanical engineering department in 2005 and 2007, respectively. Since August 2007, he has participated in the PhD program at the Centre for Ships and Ocean Structures (CeSOS) at the Norwegian University of Science and Technology, in Trondheim, Norway. His research is related to nonlinear stochastic dynamic structural response analysis of multibody structural systems, such as floating wind turbines and wave energy converters.